Supporting information

p-Phosphonic acid calix[8]arene mediated synthesis of ultralarge, ultrathin, single-crystal gold nanoplatelets

Wenzhe Zang,[a,c] Jeremiah Toster,[a] Biswanath Das,[b] Richard Gondosiswanto,[b] Shiyang Liu,[b] Paul K. Eggers,[a] Chuan Zhao,[b]* Colin L. Raston[a]* and Xianjue Chen[b]*

[a] Flinders Institute for NanoScale Science & Technology, College of Science and Engineering, Flinders University, Adelaide, SA 5001, Australia

[b] School of Chemistry, University of New South Wales, Sydney, NSW 2052, Australia

[c] Current address: Department of Electrical Engineering and Computer Science, University of Michigan, 1301 Beal Ave., Ann Arbor, Michigan 48109, United States

Email: correspondence and requests for materials should be addressed to X.C. (xianjue.chen@unsw.edu.au)

Experimental methods:

p-H_2O_3P-calix[n]arene was synthesised following the literature method (*New J. Chem.*, 2008, **32**, 1478). A mixed solution containing 0.8 mM $HAuCl_4$ with 0.2 mg mL^{-1} *p*-H_2O_3P-calix[n]arene, n = 4,5,6,8, was bubbled with hydrogen gas for 1 h. The solution was then incubated for 10 h at room temperature. The red-brick colour sediment was collected and washed using high-speed centrifuge (30 min, 16800 × *g*) with Milli-Q water for three times. Gentle bath sonication was applied to re-disperse the slurry before each centrifuge. The washed products were used directly for characterisations. The Au platelets were dropcast onto 200 mesh holey carbon copper grids followed by evaporation in air for TEM and SEM characterisations. JEOL 3000F, 2100 and F200 TEMs, operating at 300 kV, 120 kV and 200 kV, respectively, were used for TEM imaging. SEM images were acquired using FEI Nova NanoSEM 450. Image J software was used for processing all the TEM and SEM images. A NanoMan AFM system (Veeco Instruments Inc.) was used for AFM characterisation and tapping mode was used for the height profile measurement. The sample was prepared by drop casting Au platelets onto freshly cleaved mica. The raw data was processed using the Gwyddion software. ^{31}P NMR was performed on Bruker Avance III 400 MHz and 162 MHz spectrometers respectively. UV-vis measurement was carried out on a Cary 100 Bio double-beam UV-visible spectrophotometer. XRD (Panalytical MPD) pattern was analysed using X’Pert HighScore Plus software.

The as-prepared **Au-8** was deposited onto glassy carbon electrode. 5 µL of 1-butyl-1-methylpyrrolidinium bis(trifluoromethylsulfonyl)imide, ([BMP][Ntf2]) (98%, from Io-li-tech) was drop-casted onto the glassy carbon electrode. Platinum wire and silver wire was connected to the ionic liquid (IL) droplet as the counter and reference electrode, respectively. All electrochemical experiments were conducted at room temperature using a CHI760 potentiostat (CHI Instrument, Texas). Briefly, the oxygen and nitrogen (carrier) gas was flowed through digital flowmeters, to a mixing chamber and the gas sensing chamber. Prior to any measurement, the IL droplet was purged with pure nitrogen for 4 h to remove any residual atmospheric gases and water vapour. Chronoamperometric was used for detecting the oxygen gas with potential held at diffusion limited region (E = -1.2 V vs Ag wire). Different measurement of oxygen gas with concentration of 5% to 30% was conducted with 150s interval between each concentration to obtain the background current.

Supplemental figures:

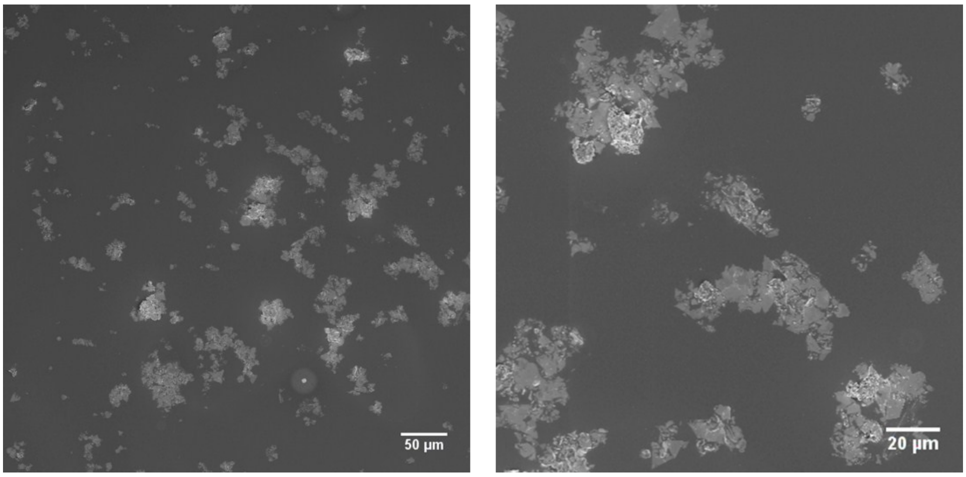

Fig. S1 Low magnification SEM images of **Au-8**.

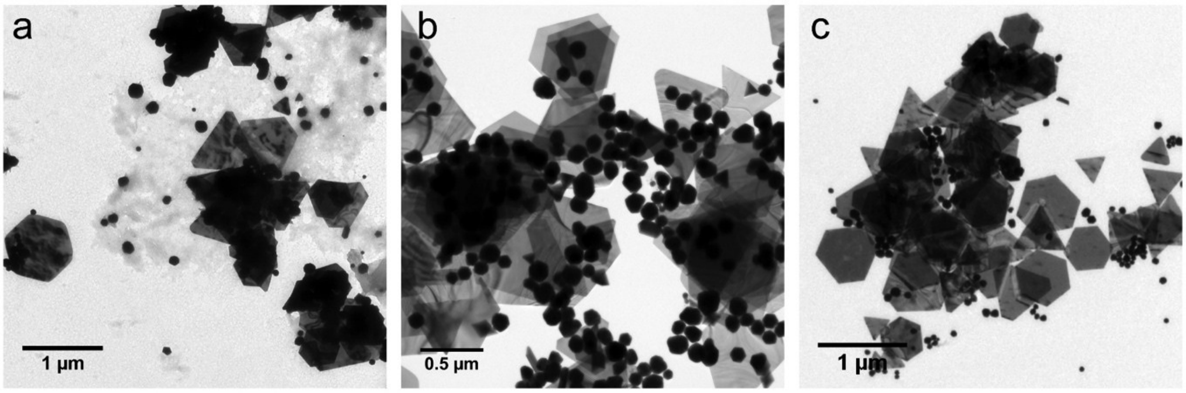

Fig. S2 TEM images of the Au sediments from (a) *p*-H_2O_3P-calix[4]arene, (b) *p*-H_2O_3P-calix[5]arene, and (c) *p*-H_2O_3P-calix[6]arene.

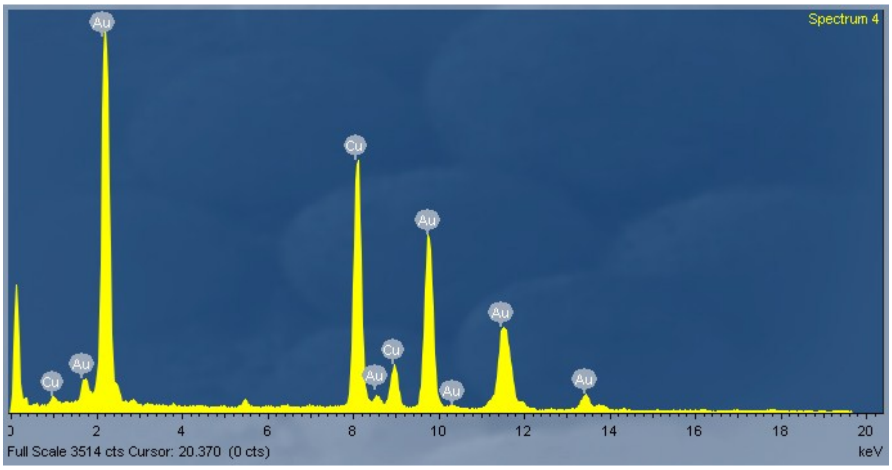

Fig. S3 EDS in TEM shows a strong signal for gold, suggesting the platelets are made of gold. The Cu signal is from the TEM Cu grid.

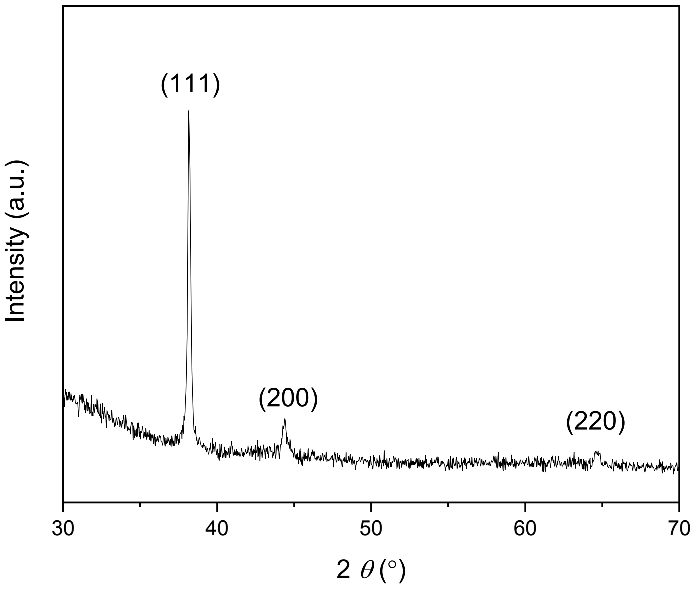

Fig. S4 XRD pattern of **Au-8**.

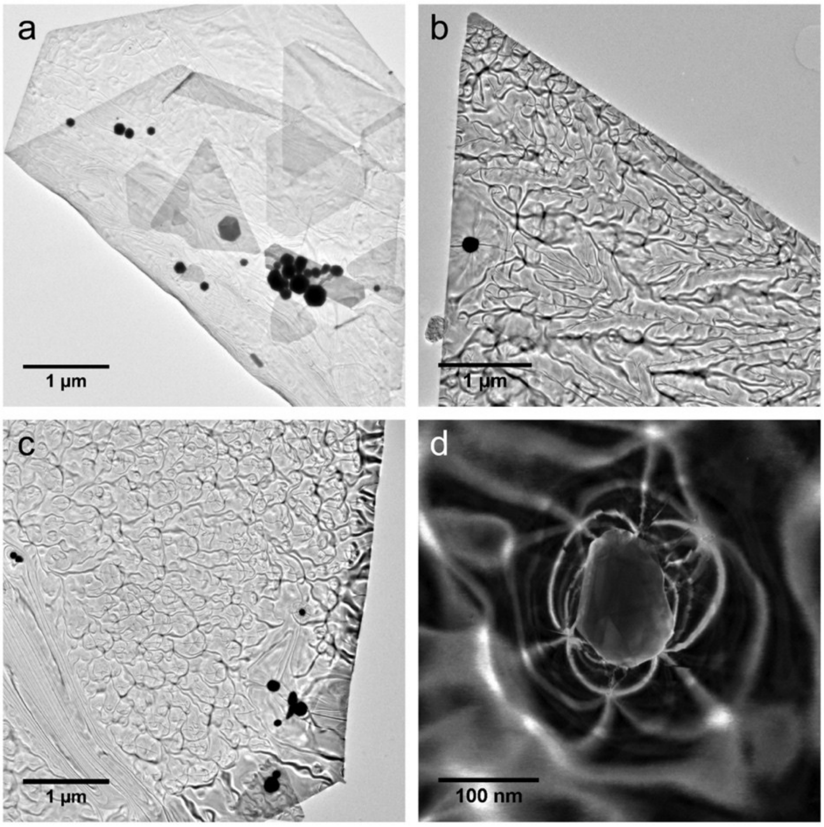

Fig. S5 TEM images showing folding and buckling of the Au platelets due to their extreme thinness. A dark-field scanning TEM image in (d) shows an Au particle sitting on top of an ultrathin platelet.

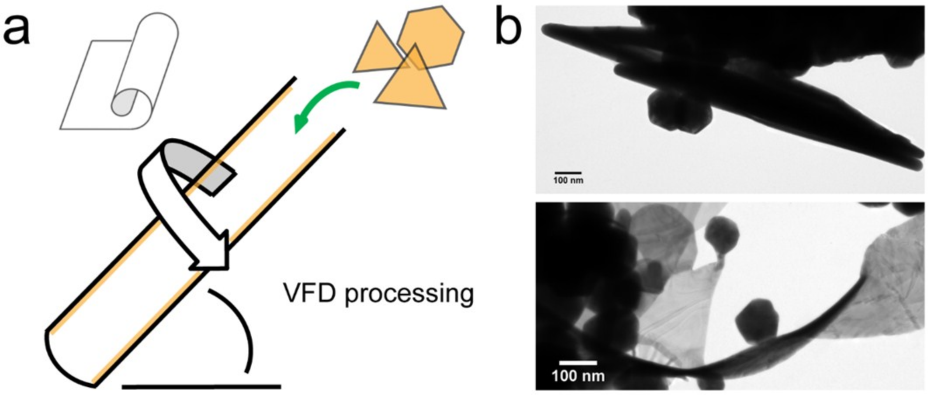

Fig. S6 (a) Schematic of the VFD processing for making of Au scrolls from platelets. (b) TEM images of the scrolled Au platelets.

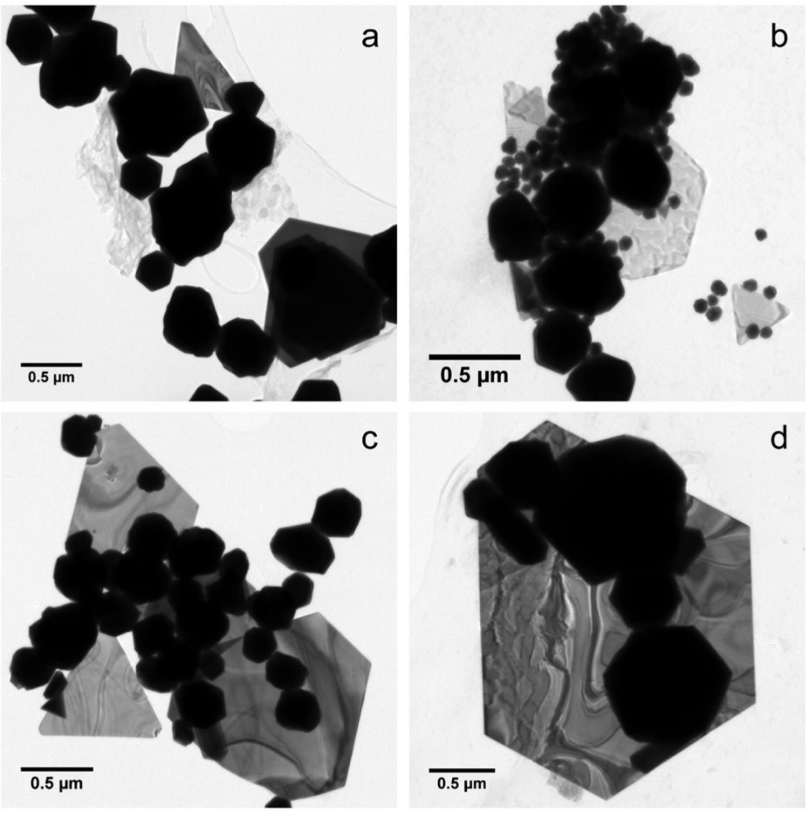

Fig. S7 TEM images of the sediments synthesised by direct mixing of $HAuCl_4$ with (a) *p*-H_2O_3P-calix[4]arene, (b) *p*-H_2O_3P-calix[5]arene, (c) *p*-H_2O_3P-calix[6]arene or (d) *p*-H_2O_3P-calix[8]arene without bubbling hydrogen.

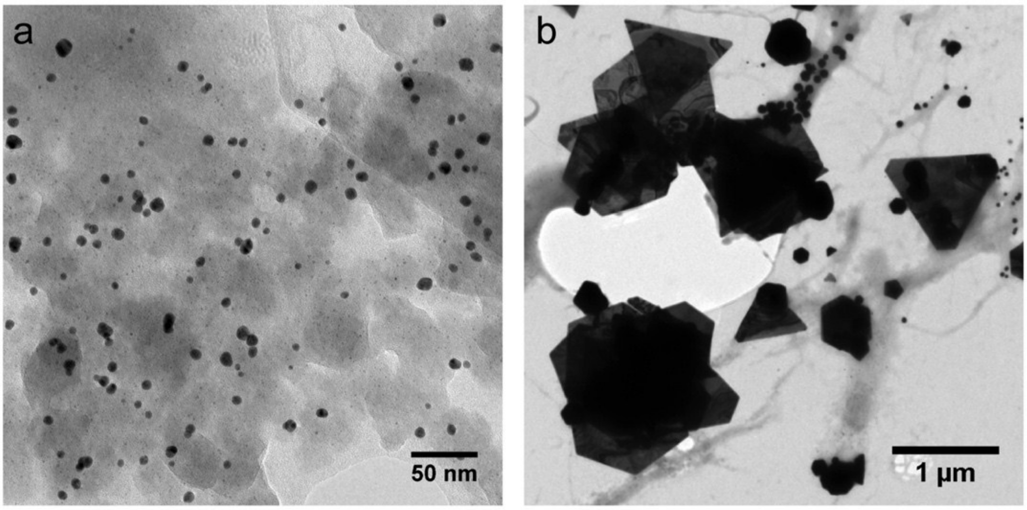

Fig. S8 TEM images showing (a) Au nanoparticles <20 nm in size formed when the concentration of *p*-H_2O_3P-calix[8]arene is 0.05 mg mL^{-1}, and (b) small Au platelets when the concentration is 0.4 mg mL^{-1}.

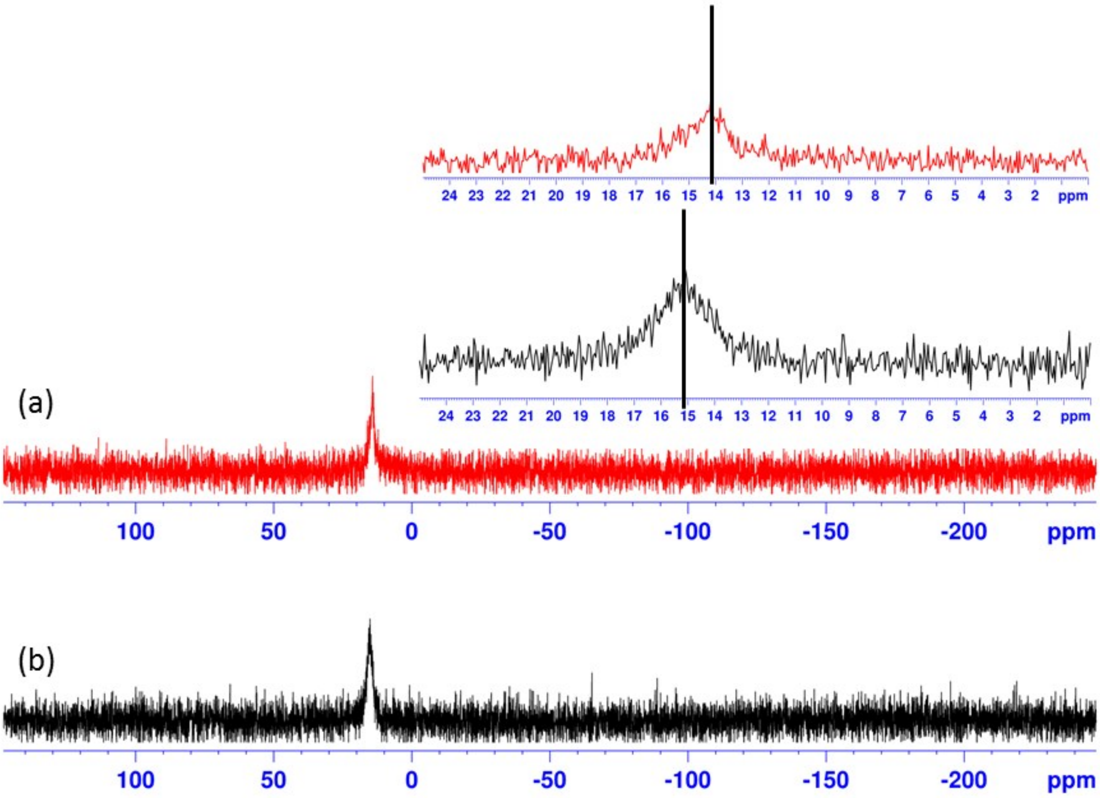

Fig. S9 162 MHz ^{31}P NMR spectra of (a) *p*-H_2O_3P-calix[8]arene (1 mM) in water and (b) *p*-H_2O_3P-calix[8]arene (1 mM) + $HAuCl_4$ (1 mM) in water. Inset shows the shift (~1.15 ppm) in the characteristic ^{31}P signal upon addition of $HAuCl_4$. Each spectrum was acquired after shimming and recording the 400 MHz ^1H NMR spectrum using suppression of the H_2O solvent signal (at δ 4.79) first.

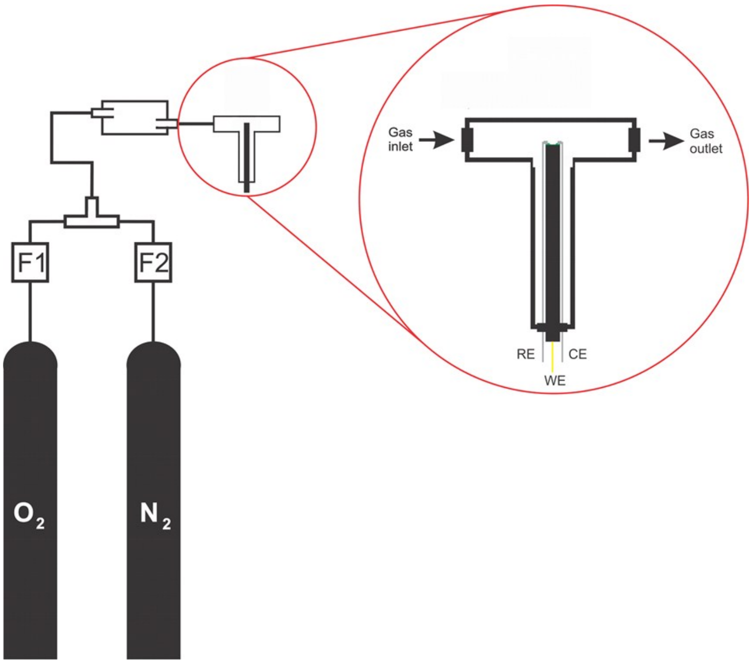

Fig. S10 Gas sensor set up. F1 and F2 are digital flow metres.

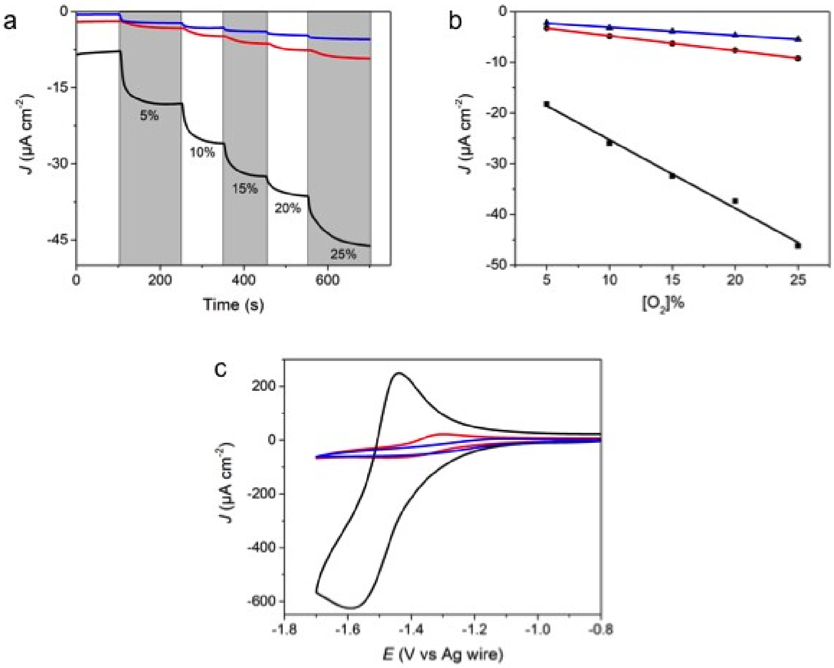

Fig. S11 The oxygen gas sensing performance of Au platelets synthesised using *p*-H_2O_3P-calix[8]arene (black line), mixture of Au particles and smaller platelets (red line) from *p*-H_2O_3P-calix[4]arene (**Fig. S2a**), and Au nanoparticles (blue line) made from a 0.05 mg mL^{-1} of *p*-H_2O_3P-calix[8]arene (**Fig. S8a**). From the (a,b) gas sensing and (c) oxygen reduction reaction performance, it is clear that the Au platelets outperform the other two samples. This could be due to the larger electro-active surface area with ultrathin platelets compared to particles.